RANS closure approximation by artificialneural networks

Andrea Ferrero, Angelo Iollo, Francesco Larocca

RANS CLOSURE APPROXIMATION BY ARTIFICIAL NEURAL NETWORKS

A. Ferrero[1] - *A. Iollo*[2] - *F. Larocca*[3]

[1] DIMEAS, Politecnico di Torino, Torino, Italy, andrea_ferrero@polito.it
[2] INRIA and Institut de Mathématiques de Bordeaux, Talence, France, angelo.iollo@inria.fr
[3] DIMEAS, Politecnico di Torino, Torino, Italy, francesco.larocca@polito.it

ABSTRACT

Turbulence modelling remains a challenge for the simulation of turbomachinery flows. Reynolds Averaged Navier-Stokes (RANS) equations will still be used for high-Reynolds number flows for several years and so there is interest in improving their prediction capability. Machine learning techniques offer several strategies which could be exploited for this purpose.

In this work, an approach to improve the Spalart-Allmaras model is investigated. In particular, the model is used to predict the flow around the T106c low pressure gas turbine cascade. As a first step, an Artificial Neural Network (ANN) is trained on the data generated by the original model. Then, an optimisation procedure is applied in order to find the weights of the network which minimise the error between the predicted results and the available experimental data. The new model is tested at different Reynolds numbers on the T106c cascade and on a wind turbine airfoil in post-stall conditions. Significant improvements are observed in the condition chosen for the optimisation. Future work will be devoted to the generalisation of the approach by including multiple working conditions optimisations and adding new physical variables as inputs of the ANN.

KEYWORDS

RANS, MACHINE LEARNING, TURBOMACHINERY

NOMENCLATURE

β_2 flow exit angle
$\chi = \hat{\nu}/\nu$ normalised turbulent viscosity
ν, $\hat{\nu}$ molecular and turbulent kinematic viscosity
ρ density
σ, c_{b1}, c_{b2}, c_{t3}, c_{t4} SA model constants
ζ kinetic losses
c, c_x chord and axial chord
$f(\chi)$ generalised production term multiplier
f_{t1} trip term
f_{t2} term to delay transition
$\boldsymbol{u}$ speed
t time
x spatial coordinate
P, D production and destruction terms
Re_{2s} isentropic exit Reynolds number
$\hat{S}$ modified vorticity

INTRODUCTION

Turbulence modelling is a key aspect in the study of turbomachinery flows since turbulence phenomena influence deeply the performance of turbines and compressors. In the last years, Large Eddy Simulation (LES) approaches were adopted to directly simulate the largest scales of turbulence by limiting the modelling effort to the smallest (and less problem-dependent) scales. This strategy can give very good results in the presence of separation and transition phenomena. However, the computational cost required by LES is so high that they are applied mainly to the study of low Reynolds number flows in simple configurations (like for example cascade flows). More complex parametric studies focused on the analysis of several stages would be prohibitive for the LES approach.

Even if the available computational power is growing quickly, this limit will remain for several years. For this reason, Reynolds Averaged Navier-Stokes (RANS) equations will remain a valid alternative to LES due to their significantly lower cost. RANS models describe the averaged field quantities which are sufficient for the prediction of several parameters of interest. However, the reliability on the prediction of these averaged quantities is strongly problem-dependent: the presence of transition or separation phenomena represents a significant challenge for RANS models.

These considerations motivate the research effort which has been devoted to the improvement of RANS closure models in the last years. Recently, some approaches based on machine learning techniques were proposed. The main idea of these strategies is to exploit the available data (experimental or numerical from high-fidelity simulations) to obtain or improve RANS turbulence closure.

For example, Wang et al. (2017) proposed a strategy to correct the errors in RANS modelled Reynolds stresses by using a data-driven physics-informed machine learning approach trained on Direct Numerical Simulation data. An approach which shares the same spirit was proposed by Mohebujjaman et al. (2019) who investigated the use of data-driven corrections for the improvement of reduced order models of fluid flows.

Another approach was proposed by Raissi and Karniadakis (2018) who used machine learning techniques to identify the governing partial differential equation which is hidden in a set of high-fidelity data with applications to the Navier-Stokes equations. Finally, Gibou et al. (2018) discussed the use of deep learning strategies in the simulation of multiphase flows.

A general strategy to improve existing RANS models was proposed by Parish and Duraisamy (2016) and Singh et al. (2017). Their approach is based on two steps: field inversion and machine learning. The field inversion step requires to introduce a spatially varying correction factor in the source term of the turbulence model. An optimisation procedure is then used to determine the correction factor distribution which minimises the prediction error on a goal function for which some experimental data are available. The optimisation is performed by means of a quasi-Newton algorithm and the gradient is evaluated by the discrete adjoint approach.

The second step of the procedure requires the use of an Artificial Neural Network (ANN) which allows to establish a functional relation between some flow features (relative turbulence intensity, vorticity, ...) and the correction factor. In this way it is possible to generalise the correction factor and use it to predict the flow field in new configurations.

This approach is very powerful because it allows to improve an existing RANS model starting from a few experimental data (even an integrated quantity, like the lift coefficient could be used). However, the price to pay is huge: the dimension of the optimisation problem which

has to be solved in the first step is given by the number of grid points. Even in 2D simulations this value is very high ($10^4 - 10^5$) and so the solution of the optimisation problem is challenging.

In this work, an alternative strategy is investigated. In particular, the focus is on the one-equation Spalart-Allmaras (SA) model. The idea is to substitute the original production term in the SA equation with an ANN which works with the same input variables as the original source term. First of all, the neural network is trained on the data produced by the original model in order to reproduce its behaviour. Secondly, an optimisation procedure is applied to the weights of the neural network in order to minimise the error between a predicted goal function and the experimental data. Since the neural network is general enough to reproduce a large family of different functions, the optimisation will explore new relations which could perform better than the original source term.
The key advantage of this approach with respect to the strategy proposed by Parish and Duraisamy (2016) and Singh et al. (2017) is that the dimensionality of the optimisation problem is significantly reduced: it is no more linked to the number of grid points but is determined by the number of connections in the neural networks which are in the order of $10^1 - 10^2$. In this preliminary work, the optimisation is performed in a single working condition. Future work will be devoted to a generalisation of this approach: the final goal is to optimise the model on several working conditions and then identify some physical quantities which can be introduced as input in the neural network in order to adapt the model to the different working conditions.

The proposed approach is applied to the simulation of the flow field around the T106c low pressure gas turbine cascade. At low Reynolds numbers the flow is dominated by laminar separation followed by transition and represents a challenge for RANS models. The neural network obtained by the proposed procedure is tested on the T106c cascade at different Reynolds numbers and on a wind turbine airfoil in post-stall conditions in order to verify the capability of the model to predict flows which are different from the one used for training and optimisation.

PHYSICAL MODEL AND DISCRETISATION

SA model

In this work the Spalart-Allmaras (SA) turbulence closure in compressible form is adopted following Allmaras and Johnson (2012). The transport equation for the modified turbulent viscosity $\hat{\nu}$ is:

$$\frac{\partial \rho\hat{\nu}}{\partial t} + \nabla \cdot (\rho \boldsymbol{u}\hat{\nu}) = \rho(P - D) + \frac{1}{\sigma}\nabla \cdot (\rho(\nu + \hat{\nu})\nabla\hat{\nu}) + \frac{c_{b2}}{\sigma}\rho(\nabla\hat{\nu})^2 - \frac{1}{\sigma}(\nu + \hat{\nu})\nabla\rho \cdot \nabla\hat{\nu} \quad (1)$$

The production term P is given by:

$$P = c_{b1}\,(1 - f_{t2})\,\hat{S}\hat{\nu} \quad (2)$$

where the modified vorticity magnitude $\hat{S}$ is defined according to Allmaras and Johnson (2012). The term f_{t2} is a function of the ratio $\chi = \hat{\nu}/\nu$:

$$f_{t2} = c_{t3} \exp\left(-c_{t4}\chi^2\right) \quad (3)$$

The term f_{t2} is introduced in the model in order to delay transition. This is necessary when the trip term f_{t1} (not included in Eq. 1) is used in order to impose transition in a certain location.

For this reason, several authors ignore the term f_{t2} when the trip term f_{t1} is not used. According to Rumsey (2007), the effects of the term f_{t2} are negligible at high Reynolds numbers and for high inlet turbulence levels. In the following the trip term f_{t1} will not be used since, in general, the location of the transition point is not known a-priori. However, the effects of the f_{t2} term on the prediction of the considered flow field will be investigated.

Numerical discretisation

The compressible RANS equations are integrated with the method of lines by using a second order accurate discontinuous Galerkin spatial discretisation and an implicit linearised Euler time integration. The discontinuos Galerkin method allows to describe complex geometries and simplifies the implementation of adaptive schemes (see for example Ferrero and Larocca (2017)) and reduced order models (Ferrero et al. (2018)). The convective fluxes are computed according to Pandolfi (1984) while the diffusive fluxes are approximated by a recovery-based scheme following Ferrero et al. (2015). The solution inside each element is described by an orthonormal modal basis obtained by the application of the modified Gram-Schmidt procedure to a set of monomials defined in the physical space, following Bassi et al. (2012). In order to speed-up the simulation, large time steps are adopted: in order to prevent some instabilities which can appear at the beginning of the simulation, a feedback filtering approach is used to prevent unphysical values following the approach proposed by Ferrero and Larocca (2016). Steady solutions are obtained by a time-marching approach in which the CFL number is controlled by a procedure which increases the time step size as the residuals decrease, following the pseudo-transient continuation strategy proposed by Bassi et al. (2010). The spatial domain is discretised by means of the Gmsh tool (see Geuzaine and Remacle (2009)) which allows to generate the parabolic curvilinear elements required by the chosen second order discretisation.

1 RANS SIMULATION OF THE T106C CASCADE

The T106c cascade is representative for high-lift profiles in low pressure gas turbines of modern aero-engines. The cascade was experimentally studied by Michaalek et al. (2012). In particular, there are experimental data on the wall isentropic Mach number (M_{is}) distribution (Hillewaert et al. (2013)) and the mass average kinetic losses (Babajee (2013)) at Reynolds numbers in the range $8 \cdot 10^4 \leq Re_{2s} \leq 2.5 \cdot 10^5$. The isentropic exit Mach number is 0.65. The inlet turbulence level intensity is very low (0.9%). The inlet angle is $32.7°$. The data show that the flow field is characterised by laminar separation which is followed by transition to turbulence in the separation region. The configuration of the flow changes when the Reynolds number is around 10^5: for lower Reynolds numbers there is a open separation while for larger Reynolds numbers there is a separation bubble after which the flow reattaches. Several RANS studies have been performed on this test case (see for example Kalitzin and Iaccarino (2002), Pacciani et al. (2011), Babajee (2013), Marty (2014), Minot et al. (2015), Ampellio et al. (2016), Ferrero et al. (2017)). The results available in the literature differ significantly from one RANS model to the other and seem to be quite sensitive to the calibration of the model. This test case was also proposed for LES and DNS simulations at two recent workshops on high-order CFD methods (see the results summary by Hillewaert et al. (2013) and Hillewaert and Galbraith (2018)).

The mesh reported in Figure 1 is used to study the flow in the T106c cascade. It is based on a structured region close to the wall surrounded by an unstructured region. It contains 6895 ele-

ments. Since the second order discontinuous Galerkin scheme introduces 3 degrees of freedom inside each element this discretisation is equivalent to a second order accurate finite volume simulation with 20685 elements. This mesh was chosen after a grid convergence study performed at $Re_{2s} = 8 \cdot 10^4$ and $Re_{2s} = 2.5 \cdot 10^5$: the same mesh will be used for all the following simulations. In order to simulate the low inlet turbulence level the inlet value of χ is set to 0.1.

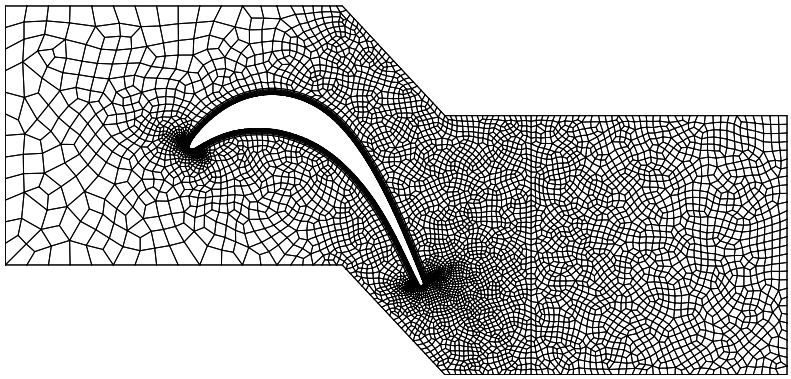

Figure 1: **Computational mesh with both structured and unstructured regions**

Sensitivity on the f_{t2} term

A preliminary study on the effects induced by the f_{t2} term is performed at $Re_{2s} = 8 \cdot 10^4, 1.2 \cdot 10^5, 1.6 \cdot 10^5, 2.5 \cdot 10^5$. The plots in Figure 2 shows the wall isentropic Mach number distribution for the standard SA model ($c_{t3} = 1.2$), for the SA model without the f_{t2} term ($c_{t3} = 0$) and for the SA model with an enhanced f_{t2} term ($c_{t3} = 2.4$). The plot also shows the experimental data obtained by the VKI and reported by Hillewaert et al. (2013). It is clear that the term f_{t2} introduces a significant effect in these simulations. Its behaviour can be put in evidence by comparing the Mach and turbulent viscosity fields obtained with the different versions of the model: Figure 4 shows clearly that the model without the f_{t2} term does not predict the separation which should be observed according to the experimental data. The plot shows that, as c_{t3} is increased the separation becomes larger and the turbulent phenomena in the wake becomes stronger. The test with $c_{t3} = 2.4$ introduces limited improvements with respect to the standard SA version ($c_{t3} = 1.2$). Further tests with a larger value ($c_{t3} = 3.6$) show some instability problems.
This preliminary study suggests to search for more general forms of the production term and puts in evidence the importance of the f_{t2} term for low Reynolds number flows.

ANN-BASED PRODUCTION TERM

The flow under study is dominated by transition phenomena. A classical way to deal with transition in RANS models is to introduce an intermittency function which alters the production term of the model. Furthermore, the preliminary study reported in the previous Section suggests that significant benefits could be obtained by acting on the production term of the SA model. For these reasons, the attention will be focused on the first part of the production term ($f(\chi) = c_{b1}\,(1 - f_{t2})$) which can be seen as a general function of χ:

$$P = f(\chi)\hat{S}\hat{\nu} \tag{4}$$

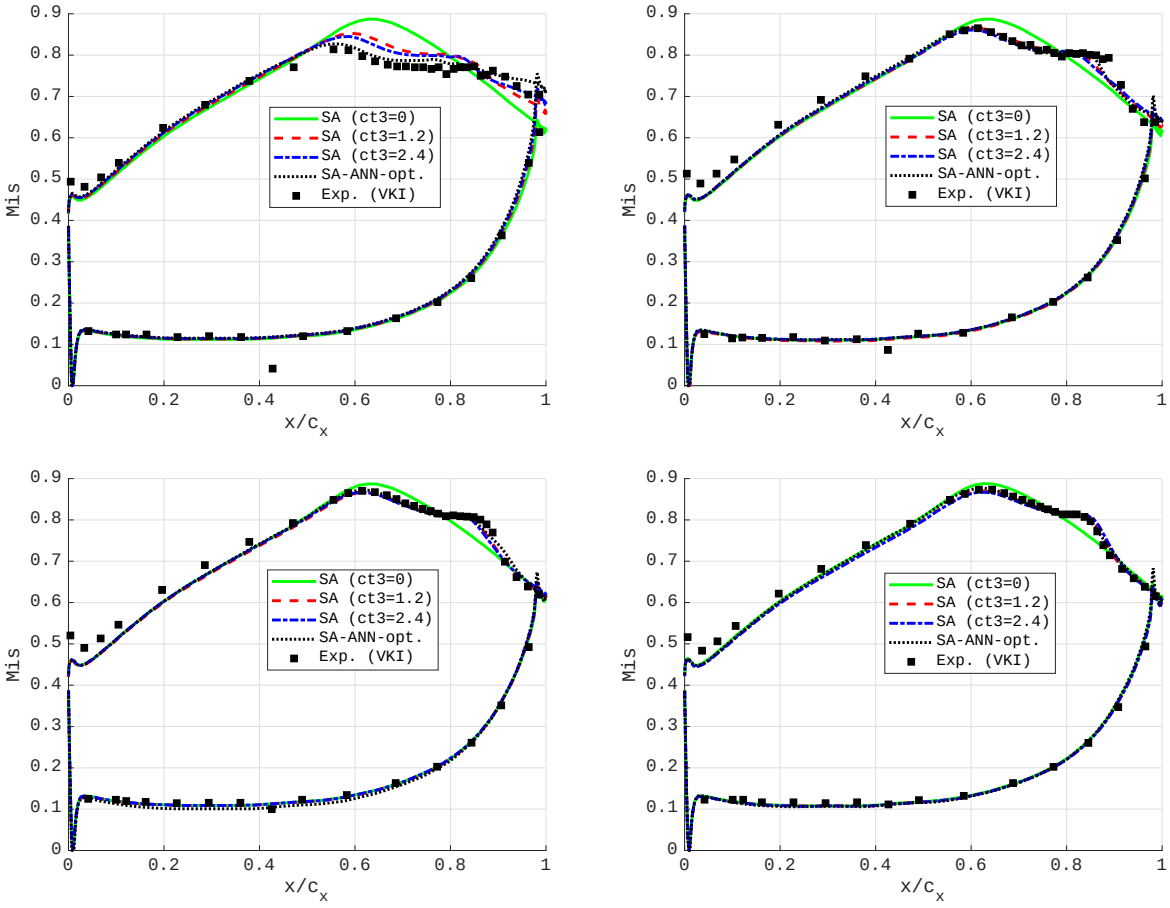

Figure 2: **Wall isentropic Mach number distribution at** $Re_{2s} = 8 \cdot 10^4, 1.2 \cdot 10^5, 1.6 \cdot 10^5, 2.5 \cdot 10^5$ **(left to right and top to bottom)**

This is in line with the approach followed by Tracey et al. (2015) who reproduced the Spalart-Allmaras source terms by means of an ANN. In the following, the function $f(\chi)$ will be described by an ANN: the capability of the neural network to describe a wide class of functions will be exploited to search new forms for the term $f(\chi)$.

The neural network

The FANN library developed by Nissen (2003) is used to describe a very simple ANN which can represent the term $f(\chi)$ with sufficient generality. The chosen architecture is very simple and has one hidden layers which two neurons. A sketch of the network is reported in Figure 3 in which neurons and biases are represented by circles and squares, respectively. Sigmoid and linear relations are chosen as activation functions for neurons in the hidden layers and output layer, respectively. The network is characterised by the presence of four connections and three biases which means that the ANN is completely defined by seven weights.
The chosen architecture was selected as the smallest one which has more parameters than the analytical correlation $f(\chi)$ (which requires four parameters: c_{b1}, c_{t3}, c_{t4} and the exponent of χ). The number of parameters in the network and the fact that the activation functions of the neurons

are strongly non-linear make the network quite general with respect to the original correlation. Some preliminary tests showed that this architecture is capable of approximating the original $f(\chi)$ as shown by Figure 3 where the original correlation is compared with the fitting obtained by training the ANN on the original correlation. Preliminary tests showed that the fitting is greatly simplified by the introduction of a logarithmic scaling on the variable χ. All the results reported in this work are obtained by using the modified variable $\tilde{\chi} = \log(\chi + \epsilon)$ as input for the ANN, where $\epsilon = 10^{-5}$ is introduced to deal with the points where the eddy viscosity is zero. The initial training is performed on a database defined by considering the data in all the grid points obtained by a simulation with the standard SA model ($c_{t3} = 1.2$) of the T106c cascade at $Re_{2s} = 8 \cdot 10^4$. The data could also be obtained directly by the analytical correlation. However, the simulation is useful to understand the range of values spanned by the variable χ in the considered class of problems. The training is performed with the modified RPROP algorithm (Igel and Hüsken (2000)) and setting a tolerance on the mean square error of the output equal to 10^{-5}.

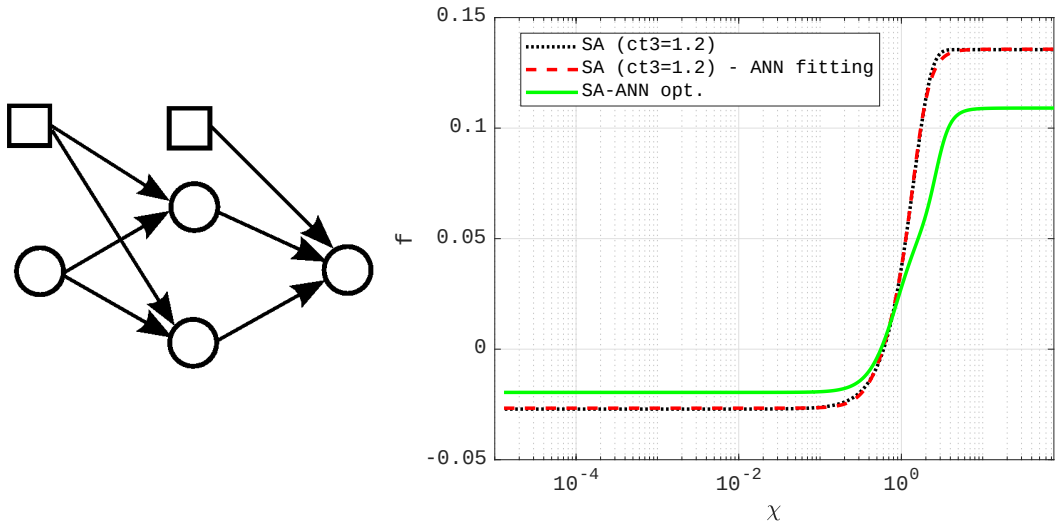

Figure 3: **ANN for the correlation $f(\chi)$ (left) and comparison between original correlation, ANN fitting of the original correlation and optimised ANN (right)**

Weights optimisation

An optimisation procedure has been developed to find weights for the ANN which give better predictions than the original model for a low Reynolds number working conditions ($Re_{2s} = 8 \cdot 10^4$). The goal function of the optimisation is represented by the mean quadratic error of the wall isentropic Mach number on the suction side evaluated in the available experimental points. The choice of this goal function is motivated by the need of showing a simple proof of concept of the proposed approach but other choices are possible. For example, the losses and the exit angle in the wake could be considered and also a weighted combination of different goal functions could be used. Furthermore, there could be an influence of the spatial distribution of the experimental points on the weight that different regions have in the definition of the goal function: if the goal function is simply evaluated as the mean quadratic error on the

experimental points then the regions in which the experimental sampling is finer give a larger contribution to the goal function.

A very simple optimisation procedure based on a gradient descent approach is implemented. The gradient is evaluated numerically by a perturbation approach. The procedure is quite expensive since each function evaluation requires to solve a steady simulation. However, each simulation is initialised by the previous steady configuration which is quite similar and so the implicit time integration scheme can perform the simulation in a reduced amount of time. The choice of using a numerical gradient evaluation was made for the sake of simplicity in order to perform a preliminary investigation of the potential of the proposed approach. A better approach would be to compute the gradient by means of an adjoint based method as done by Singh et al. (2017).
The function described by the optimised ANN is reported in Figure 3. It must be emphasised that the gradient based optimisation tends to stop in local minimum and so the obtained results could not be the best one. It would be useful to run the optimisation with different starting points.

Results

The ANN optimised for $Re_{2s} = 8 \cdot 10^4$ is used to perform predictions of the flow field around the T106c cascade for $Re_{2s} = 8 \cdot 10^4, 1.2 \cdot 10^5, 1.6 \cdot 10^5$ and $2.5 \cdot 10^5$. A significant improvement with respect to the standard SA model can be seen in the results obtained at $Re_{2s} = 8 \cdot 10^4$ (see Figures 2 and 4) while there are only small differences for larger Reynolds numbers at which the original SA model with the f_{t2} term ($c_{t3} = 1.2$) can already give good results. A detail of the suction side region close to the trailing edge for $Re_{2s} = 8 \cdot 10^4$ is reported in Figure 5: the streamlines put in evidence the shape of the recirculation region predicted by the different models.
The plots in Figure 6 shows the dependency of the mass averaged kinetic losses ζ and exit angle β_2 as a function of the Reynolds number: the obtained results are compared with the VKI experimental data reported by Babajee (2013) and with the numerical results of Pacciani et al. (2011), Benyahia et al. (2011) and Babajee (2013).
The obtained results show that the initial assumption about the need to modify the production term was reasonable. However, the ANN-SA model is here obtained by a single point optimisation and so there are no guarantees about its general validity.

In order to further investigate this point, the model optimised for the T106c at $Re_{2s} = 8 \cdot 10^4$ is also tested on the DU91-W2-250 wind turbine airfoil at $Re_\infty = 3 \cdot 10^6$, $M_\infty = 0.2$ and incidence $\alpha_\infty = 15.2^o$. In these conditions, the airfoil is characterised by a large separation as shown by the experimental results reported by Timmer and Van Rooij (2003). The flow around the airfoil is studied by means of a hybrid structured-unstructured mesh with 27001 elements and a second order accurate DG discretisation (which means that 81003 degrees of freedom per equation are introduced). A detail of the mesh is reported in Figure 7. The far field boundaries are at 20 chord lengths from the body.
The wall pressure coefficient distribution is reported in Figure 8 where the numerical predictions are compared with the experimental data. A first simulation is performed with the standard SA model ($c_{t3} = 1.2$) which gives a steady solution obtained by the pseudo-transient continuaton strategy described in Section . A second simulation is performed with the ANN-based version of the model: the results show that this version of the model is not able to fully stabilise the

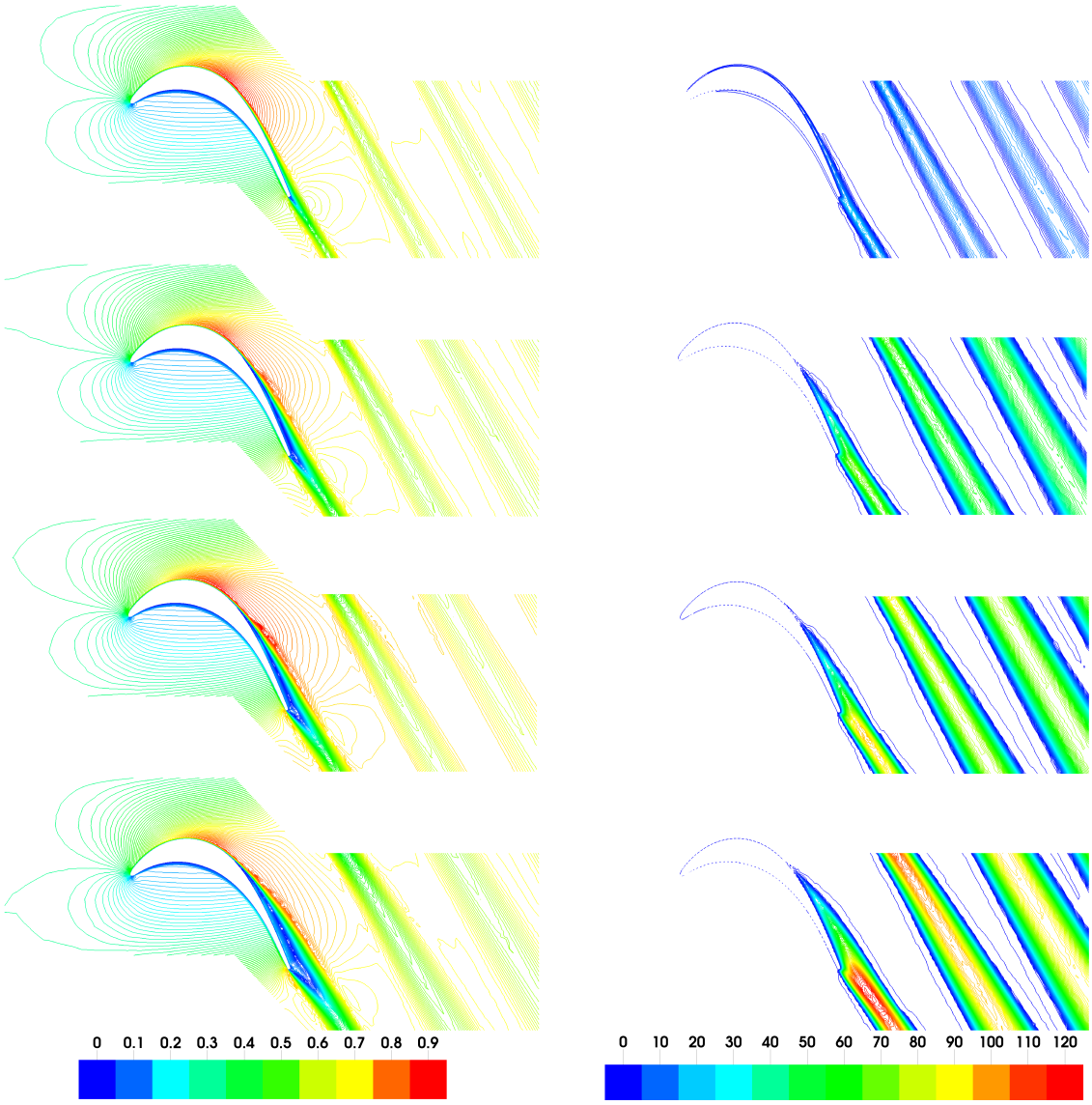

Figure 4: **Mach field (left) and normalised turbulent viscosity $\hat{\nu}/\nu$ (right) at $Re_{2s} = 8 \cdot 10^4$ with SA($c_{t3} = 0$), SA($c_{t3} = 1.2$), SA($c_{t3} = 2.4$) and SA-ANN-opt (from top to bottom)**

wake and so the solution remains unsteady with a strong vortex shedding. This is evident in Figure 9 which shows a comparison between the instantaneous field of turbulent eddy viscosity for the standard SA model at convergence (left) and the optimised ANN-based version (right). Since the equation residuals do not decrease when the ANN-based model is used, the pseudo-transient continuation strategy is deactivated and a fixed time step size is imposed in order to describe the unsteady vortex shedding. The wall pressure coefficient distribution for the ANN-based model reported in Figure 8 is obtained by time averaging.

The results show that the ANN-based version of the model produces an earlier separation with respect to the standard SA model ($c_{t3} = 1.2$): this makes the ANN-based results closer to the experimental data for what concerns the location of the separation points. However, the ANN-based model tends to underestimate the production of turbulent eddy viscosity on the pressure

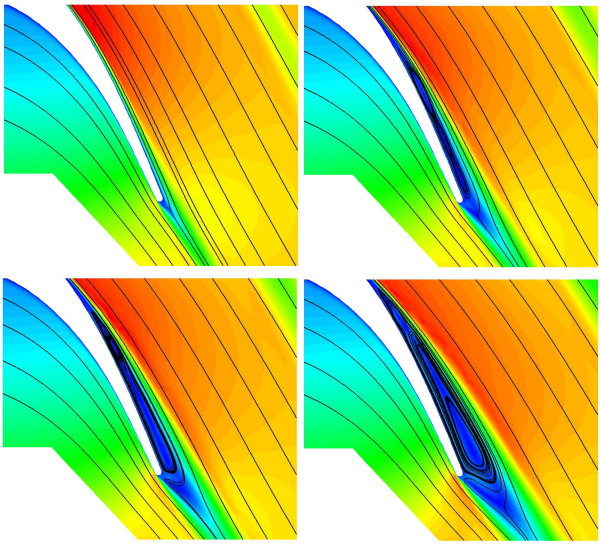

Figure 5: **Streamlines and Mach field at $Re_{2s} = 80000$ for SA with $c_{t3} = 0, 1.2, 2.4$ and SA-ANN (left to right and top to bottom)**

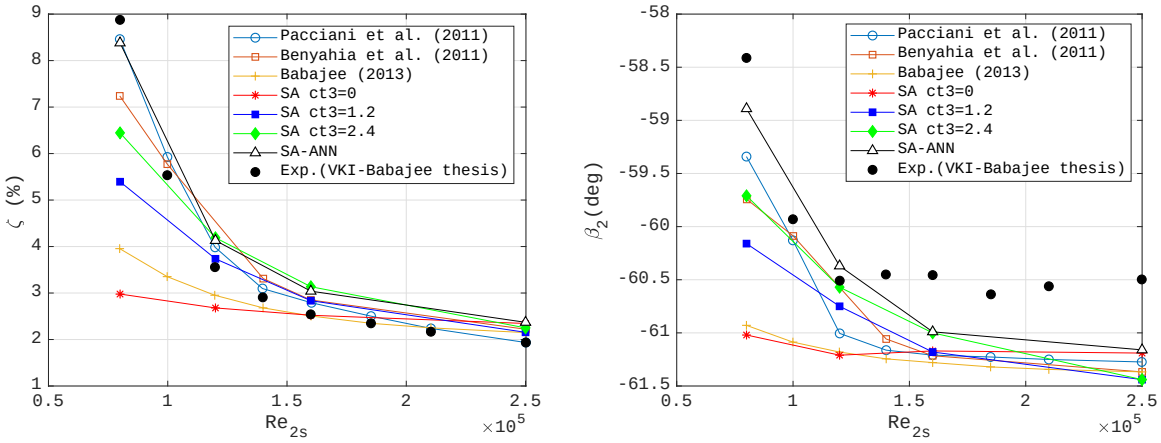

Figure 6: **Mass averaged kinetic losses (left) and exit angle (right) at different Re_{2s}**

side and leads to a small separation on the suction side which is not present in the experimental data, as can be seen in Figure 8 at $x/c = 0.6$.

CONCLUSIONS

An ANN is used to describe the production term of the Spalart-Allmaras turbulence model. The ANN is initially fitted on the original model and then the weights of the network are optimised in order to improve the agreement with the available experimental data in a certain working conditions. The procedure is applied to a low pressure gas turbine cascade characterised by laminar separation and subsequent transition to turbulence. The approach improves significantly the results with respect to the original model. The behaviour of the optimised model is investigated at different Reynolds numbers and in a completely different test case (wind turbine

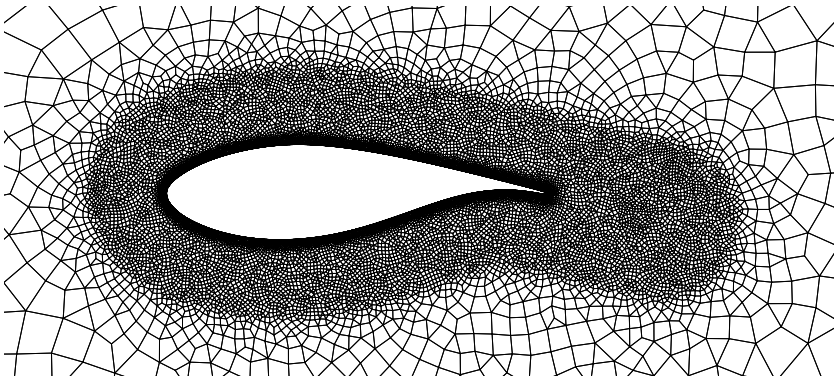

Figure 7: **Detail of the mesh for wind turbine airfoil (27001 elements)**

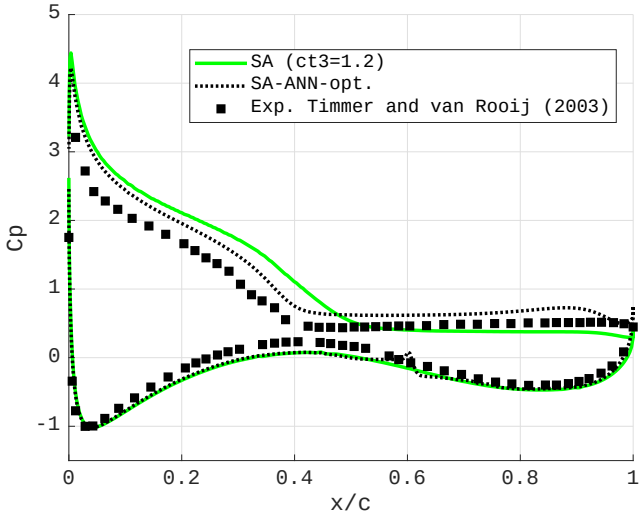

Figure 8: **Wall pressure coefficient distribution for wind turbine airfoil: original model and SA-ANN (time average) predictions**

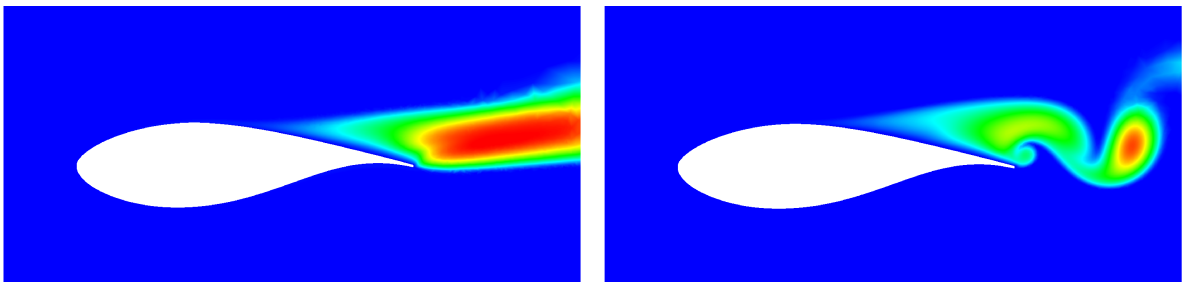

Figure 9: **Turbulent eddy viscosity field for wind turbine airfoil: original SA model at convergence (left) and unsteady SA-ANN model (right) predictions**

airfoil in post-stall conditions at $Re_\infty = 3 \cdot 10^6$).
This work represents a first step in which the optimisation of the model is performed on a single working condition. Since a single point optimisation does not give any guarantee on the validity of the model for different working conditions, the final goal is to optimise the model in several working conditions on different test cases: future work will be devoted to identify a relation between the different forms of the model obtained in the different working conditions and some physical variables which can be introduced as inputs in the neural network.

The methodology described here can be seen as an alternative to the field inversion and machine learning approach proposed by Parish and Duraisamy (2016) and Singh et al. (2017). The advantage of the present method is given by the smaller computational cost of the optimisation problem which is characterised by a number of parameters (the weights of the network) which could potentially be orders of magnitude smaller than what required by the field inversion approach (where the number of parameters is given by the number of grid points). However, the field inversion approach makes it easier to generalise the model by keeping into account data from several working conditions. It is indeed possible to invert the field for different problems and then train an ANN on the full database which includes all the cases. This is due to the fact that the approach is based on two independent steps: the field inversion process in the first step and the data-driven augmentation of the turbulence model in the second step. Furthermore, the field inversion process requires a computational cost which increases linearly with the number of test cases. In contrast, the preliminary approach proposed here is focused on the optimisation of the model on a given working conditions: the generalisation of the approach to include the data from several working points and the estimation of the cost of this process is still under investigation.
The optimisation performed in this work is based on a gradient descent method with a numerical evaluation of the gradient. These choices were made for the sake of simplicity in order to perform a preliminary investigation of the potential of the proposed approach. Future work will be devoted to reduce the cost of the procedure by implementing more efficient strategies: a possible approach would be the use of a quasi-Newton optimisation algorithm with an adjoint based gradient computation as done by Singh et al. (2017).

Acknowledgments

Computational resources were provided by HPC@POLITO (http://www.hpc.polito.it).

References

Allmaras, S. R. and Johnson, F. T. (2012). Modifications and clarifications for the implementation of the spalart-allmaras turbulence model. In *Seventh international conference on computational fluid dynamics (ICCFD7)*, pages 1–11.

Ampellio, E., Bertini, F., Ferrero, A., Larocca, F., and Vassio, L. (2016). Turbomachinery design by a swarm-based optimization method coupled with a cfd solver. *Advances in aircraft and spacecraft science*, 3(2):149–170.

Babajee, J. (2013). *Detailed numerical characterization of the separation-induced transition, including bursting, in a low-pressure turbine environment*. PhD thesis, Ecole Centrale de Lyon; Institut von Karman de dynamique des fluides (Rhode-Saint-Genèse, Belgique).

Bassi, F., Botti, L., Colombo, A., Crivellini, A., Franchina, N., Ghidoni, A., and Rebay, S. (2010). Very high-order accurate discontinuous galerkin computation of transonic turbulent flows on aeronautical configurations. In *ADIGMA-A European Initiative on the Development of Adaptive Higher-Order Variational Methods for Aerospace Applications*, pages 25–38. Springer.

Bassi, F., Botti, L., Colombo, A., Di Pietro, D. A., and Tesini, P. (2012). On the flexibility of agglomeration based physical space discontinuous galerkin discretizations. *Journal of Computational Physics*, 231(1):45–65.

Benyahia, A., Castillon, L., and Houdeville, R. (2011). Prediction of separation-induced transition on high lift low pressure turbine blade. In *ASME 2011 Turbo Expo: Turbine Technical Conference and Exposition*, pages 1835–1846. American Society of Mechanical Engineers.

Ferrero, A., Iollo, A., and Larocca, F. (2018). Global and local pod models for the prediction of compressible flows with dg methods. *International Journal for Numerical Methods in Engineering*, 116(5):332–357.

Ferrero, A. and Larocca, F. (2016). Feedback filtering in discontinuous galerkin methods for euler equations. *Progress in Computational Fluid Dynamics, an International Journal*, 16(1):14–25.

Ferrero, A. and Larocca, F. (2017). Adaptive cfd schemes for aerospace propulsion. *Journal of Physics: Conference Series*, 841(1).

Ferrero, A., Larocca, F., and Bernaschek, V. (2017). Unstructured discretisation of a non-local transition model for turbomachinery flows. *Advances in aircraft and spacecraft science*, 4(5):555–571.

Ferrero, A., Larocca, F., and Puppo, G. (2015). A robust and adaptive recovery-based discontinuous galerkin method for the numerical solution of convection–diffusion equations. *International Journal for Numerical Methods in Fluids*, 77(2):63–91.

Geuzaine, C. and Remacle, J.-F. (2009). Gmsh: A 3-d finite element mesh generator with built-in pre-and post-processing facilities. *International journal for numerical methods in engineering*, 79(11):1309–1331.

Gibou, F., Hyde, D., and Fedkiw, R. (2018). Sharp interface approaches and deep learning techniques for multiphase flows. *Journal of Computational Physics*, 380:442–463.

Hillewaert, K., Carton de Wiart, C., and Arts, T. (2013). Dns and les of transitional flow around a high-lift turbine cascade at low reynolds number. Technical report, 2nd International Workshop on High-Order CFD Methods. http://www.as.dlr.de/hiocfd.

Hillewaert, K. and Galbraith, M. (2018). Spanwise periodic dns/les of transitional turbine cascades. Technical report, 5th International Workshop on High-Order CFD Methods. https://how5.cenaero.be.

Igel, C. and Hüsken, M. (2000). Improving the rprop learning algorithm. In *Proceedings of the second international ICSC symposium on neural computation (NC 2000)*, volume 2000, pages 115–121. Citeseer.

Kalitzin, G. and Iaccarino, G. (2002). Turbulence modeling in an immersed-boundary rans method. *CTR Annual Briefs*, pages 415–426.

Marty, J. (2014). Numerical investigations of separation-induced transition on high-lift low-pressure turbine using rans and les methods. *Proceedings of the Institution of Mechanical Engineers, Part A: Journal of Power and Energy*, 228(8):924–952.

Michaalek, J., Monaldi, M., and Arts, T. (2012). Aerodynamic performance of a very high lift low pressure turbine airfoil (t106c) at low reynolds and high mach number with effect of free stream turbulence intensity. *Journal of Turbomachinery*, 134(6):061009.

Minot, A., de Saint Victor, X., Marty, J., and Perraud, J. (2015). Advanced numerical setup for separation-induced transition on high-lift low-pressure turbine flows using the γ-rθt˜ model. In *ASME Turbo Expo 2015: Turbine Technical Conference and Exposition*, pages V02BT39A010–V02BT39A010. American Society of Mechanical Engineers.

Mohebujjaman, M., Rebholz, L. G., and Iliescu, T. (2019). Physically constrained data-driven correction for reduced-order modeling of fluid flows. *International Journal for Numerical Methods in Fluids*, 89(3):103–122.

Nissen, S. (2003). Implementation of a fast artificial neural network library (fann). Technical report, Department of Computer Science University of Copenhagen (DIKU). http://fann.sf.net.

Pacciani, R., Marconcini, M., Fadai-Ghotbi, A., Lardeau, S., and Leschziner, M. A. (2011). Calculation of high-lift cascades in low pressure turbine conditions using a three-equation model. *Journal of Turbomachinery*, 133(3):031016.

Pandolfi, M. (1984). A contribution to the numerical prediction of unsteady flows. *AIAA journal*, 22(5):602–610.

Parish, E. J. and Duraisamy, K. (2016). A paradigm for data-driven predictive modeling using field inversion and machine learning. *Journal of Computational Physics*, 305:758–774.

Raissi, M. and Karniadakis, G. E. (2018). Hidden physics models: Machine learning of nonlinear partial differential equations. *Journal of Computational Physics*, 357:125–141.

Rumsey, C. L. (2007). Apparent transition behavior of widely-used turbulence models. *International Journal of Heat and Fluid Flow*, 28(6):1460–1471.

Singh, A. P., Medida, S., and Duraisamy, K. (2017). Machine-learning-augmented predictive modeling of turbulent separated flows over airfoils. *AIAA Journal*, pages 2215–2227.

Timmer, W. and Van Rooij, R. (2003). Summary of the delft university wind turbine dedicated airfoils. *Journal of solar energy engineering*, 125(4):488–496.

Tracey, B. D., Duraisamy, K., and Alonso, J. J. (2015). A machine learning strategy to assist turbulence model development. In *53rd AIAA Aerospace Sciences Meeting*, page 1287.

Wang, J.-X., Wu, J.-L., and Xiao, H. (2017). Physics-informed machine learning approach for reconstructing reynolds stress modeling discrepancies based on dns data. *Physical Review Fluids*, 2(3):034603.